Sustainability **2015**, *7*, 2804-2817; doi:10.3390/su7032804

OPEN ACCESS

sustainability

ISSN 2071-1050

www.mdpi.com/journal/sustainability

Article

Study on the Thermal Effects and Air Quality Improvement of Green Roof

Heng Luo [1,2,*], Ning Wang [2], Jianping Chen [1,2], Xiaoyan Ye [2] and Yun-Fei Sun [2,3]

[1] Jiangsu Key Laboratory of Intelligent Building Energy Efficiency, Suzhou University of Science and Technology, Suzhou 215009, China; E-Mail: alanjpchen@yahoo.com

[2] Suzhou Key Laboratory of Mobile Networking and Applied Technologies, Suzhou University of Science and Technology, Suzhou 215009, China; E-Mails: kenibote@sina.com (N.W.); ustsyxy@163.com (X.Y.); yfsun2009@sinano.ac.cn (Y.-F.S.)

[3] Suzhou Institute of Nano-Tech and Nano-Bionics, Chinese Academy of Sciences, Suzhou 215009, China

* Author to whom correspondence should be addressed; E-Mail: luoheng1981@163.com; Tel.: +86-512-6957-3006.

Academic Editor: Vincenzo Torretta

Received: 16 December 2014 / Accepted: 27 February 2015 / Published: 6 March 2015

Abstract: Heat island phenomenon and air quality deterioration issues are two major problems that have occurred during the process of urbanization, especially in developing countries. A number of measures have been proposed, among which roof greening is considered as a promising one due to its outstanding performance in thermal effects as well as air quality improvement. A self-maintenance system, termed the Green Roof Manager (GRM), which comprises the irrigation and shadowing subsystems, is proposed in this paper, focusing on the automatic and reliable operation of the roof greening system rather than exploiting new plant species. A three month long experiment was set up, resulting in the observation that a 14.7% of, on average, temperature reduction can be achieved in summer after deploying the GRM system. During a 24-hour monitoring experiment the PM2.5 concentrations above the GRM was reduced by up to 14.1% over the bare roof.

Keywords: urbanization; green roof; self-maintenance; sustainability; thermal effects; air quality

---

1. Introduction

Urbanization has been the dominant demographic trend in the whole world over the past decades and the great rural-to-urban population shift is expected to continue in the 21st century, especially in developing countries like China. Statistics released by the Ministry of Housing and Urban-Rural Development of the People's Republic of China shows that the urbanization rate was 53.73% in 2013 and this figure is expected to grow further before stabilizing at 65% within the future 20 years.

Undoubtedly, urbanization has a set of positive impacts on human beings, *i.e.*, better health care, infrastructure conditions and services. Moreover, historical evidence has also demonstrated the strong relationship between urbanization and declining birth rate, which reduces population pressure on land and nature resources. Additional job positions and robust economic growth are two more advantages.

Despite its merits, urbanization has also triggered a range of problems (e.g., air pollution issues and urban heat island phenomenon) globally. Adverse human health effects, *i.e.*, cardiovascular disease [1], pulmonary injury [2], neurodegenerative disorders [3], asthma [4] and mortality [5,6] are often associated with long-term exposure to air pollutants whose density is extremely higher in urban areas compared to rural sites. A huge amount of energy, especially in summer, is consumed in many modern cities nowadays [7,8]. These problems have seriously affected the development of modern society which is contrary to the principles of sustainable development. In spite of numerous measures being taken, environmental problems have become much more serious in recent years.

Figure 1 outlines the air quality condition across China in 2013. As seen, the air condition in developed eastern coastal areas where the urbanization rate is high is worse than that in the less developed western parts.

Urban Heat Island (UHI) is another major problem posed to human beings in the 21st century as a result of urbanization [9–11]. A great deal of energy was consumed by the HVAC system, especially in summer in the past years [12,13]. Figure 2 shows the temperature distribution around China in July 2013. As shown, urban agglomeration overlaps with the regions where temperature is comparatively high.

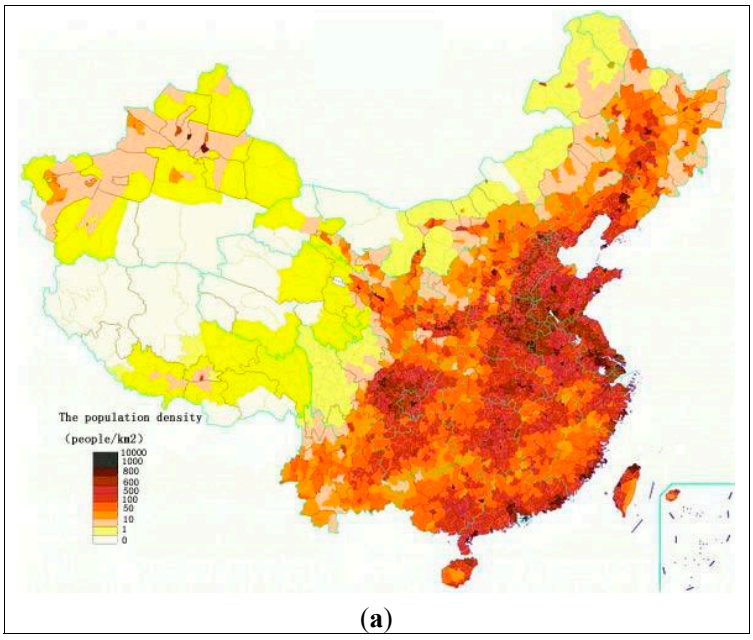

(**a**)

Figure 1. *Cont.*

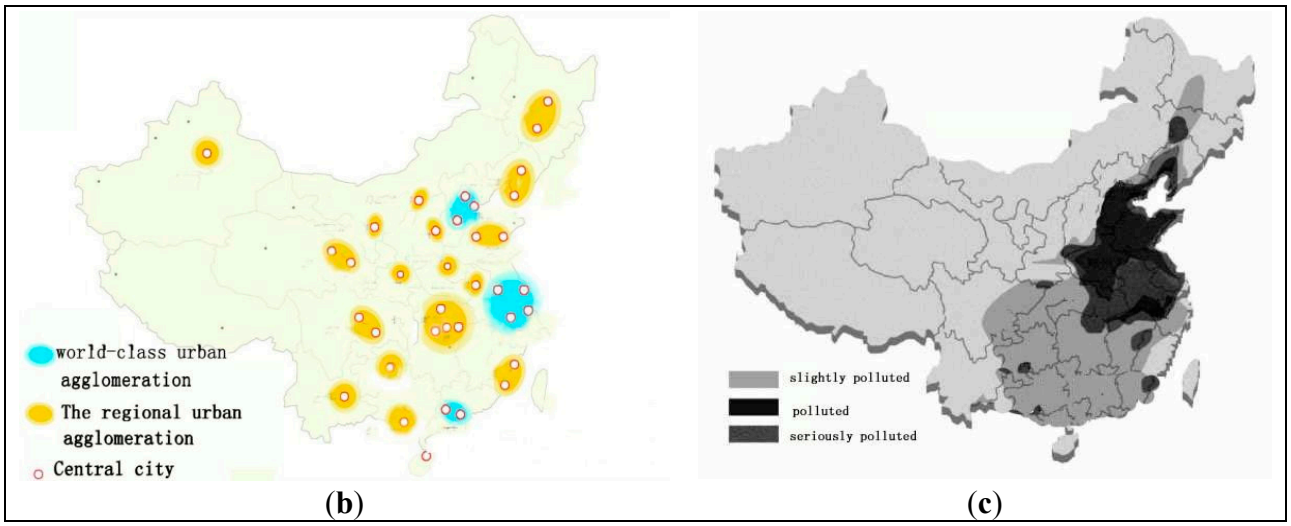

Figure 1. The relationship between AQI (Air Quality Index) and urbanization in China. (**a**) Population distribution; (**b**) Urban agglomeration distribution; (**c**) Air pollution in China.

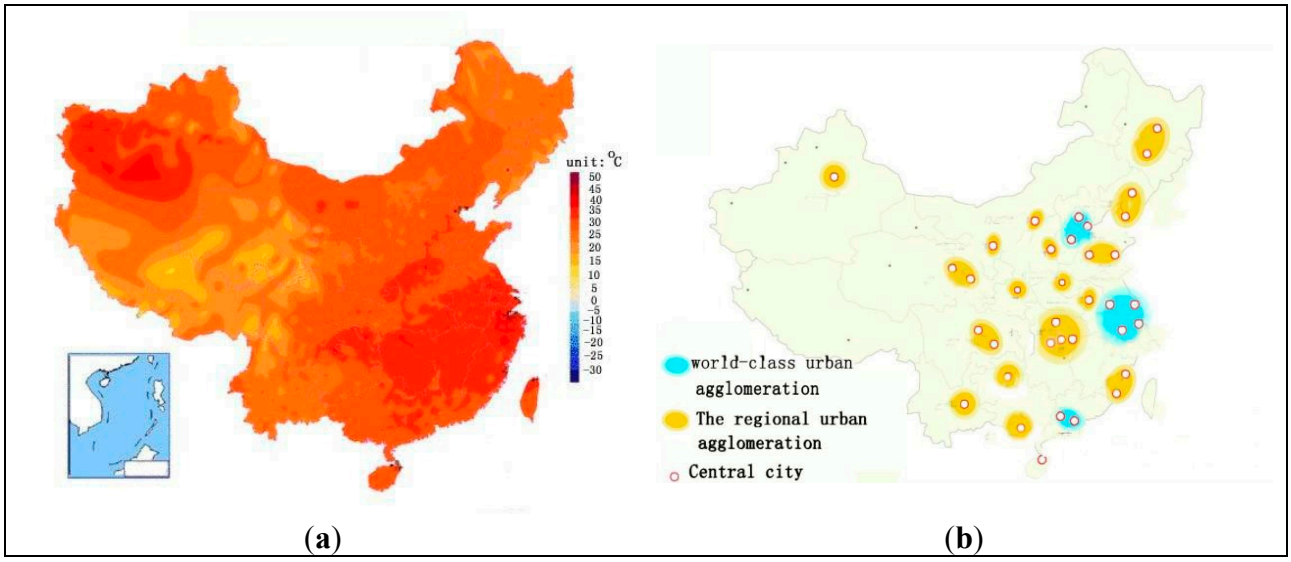

Figure 2. The relationship between temperature and urbanization in China. (**a**) Temperature distribution; (**b**) Urban agglomeration distribution.

Sustainable development has been a worldwide research focus since its emergence, leading to a large quantity of environment friendly means [14,15] among which green roof is popular [16]. It has already been demonstrated that thermal effects can be improved significantly near green roofs because of the shadowing effect caused by vegetation. Fiorettiet *et al.* report an average 90% radiation reduction beneath green roof vegetation canopies during hot seasons in Italy [17]. Besides, green roofs are capable of cleaning air [18] and buffering rain during intensive rainfall events [19]. Habitats and food sources can also be provided by green roofs for a suite of local invertebrate and bird communities [20] and biodiversity will be thus increased [21–24].

Despite the advantages brought by green roof practice, some problems (e.g., vegetation selection, management system, *etc.*) are still left unaddressed. A self-maintenance system, termed the Green Roof Manager (GRM), is thus proposed in this paper to manage the green roof system efficiently. We

distinguished ourselves in the way that the GRM focuses on the research of an adaptive and reliable maintenance system without involvement of human beings rather than exploiting the plants specie for given climate regions. The performance of the GRM is studied carefully and its ecological impact is also explored in detail in this paper.

The following second part introduces the structure of the GRM system. Section 3 and Section 4 we describe the experiment setup and results respectively and the final section concludes this paper.

2. The GRM System

The GRM system, as shown in Figure 3, is a complete self-maintenance system controlled by electrical devices. Manual control is also available when necessary. As seen in Figure 3a, all devices in this system are powered by solar energy to avoid additional energy cost and rain water is conserved for future irrigation, targeting at water consumption reduction. A series of operating parameters, *i.e.*, temperature, humility and light are measured and transmitted via the GPRS before reaching the cloud where machine learning is performed. Control command is transmitted backward to the local PCT (Point of Control and Transmission), aiming at irrigation and shadowing.

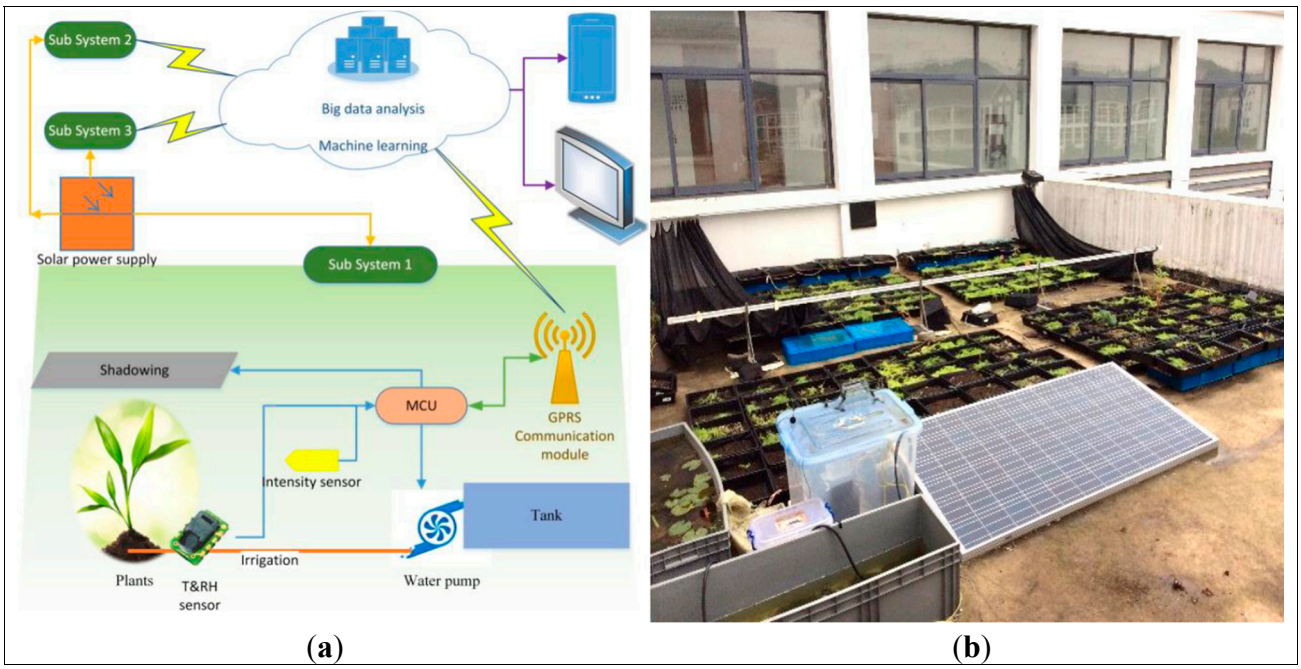

Figure 3. Self-management system. (**a**) Green Roof Manager (GRM) diagram; (**b**) GRM implementation.

2.1. Hardware Design

Figure 4 describes the hardware design of the proposed GRM system. As shown, the whole system is composed of the Data Collection Unit, the Local PCT and the Analysis unit. Environment measurements are obtained by the Data Collection Unit before being relayed to the cloud, which conducts information analysis, using data mining and machine learning techniques after which control operations are transmitted backward to the local PCT so that corresponding equipment can be controlled, aiming at irrigation and shadowing.

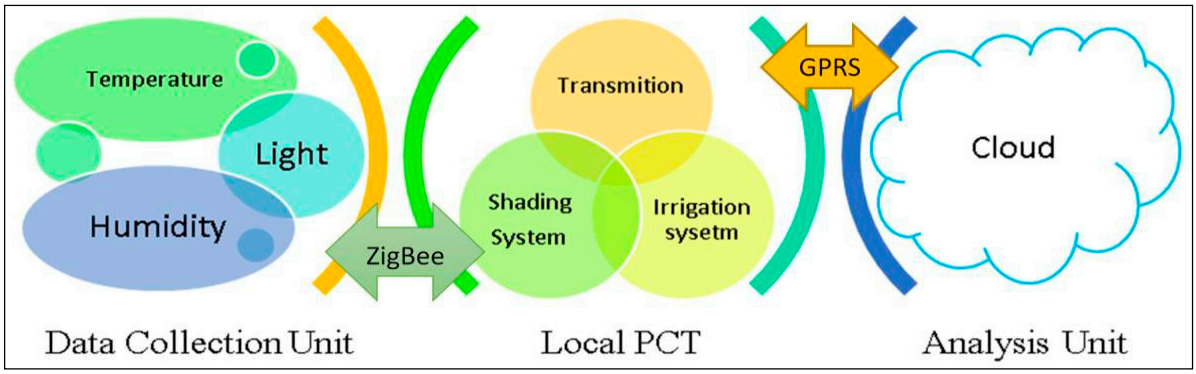

Figure 4. The structure of the system.

2.2. Software Design

The software diagram of the GRM is outlined in Figure 5. As observed, a unique ID is assigned, after initialization, to each unit to ensure precise control for corresponding equipment. Authentication is required to guarantee the safety of the GRM system. The operation parameters, together with results, will be saved in the Server for further investigation. Feedback can therefore be realized so that the GRM behave optimally.

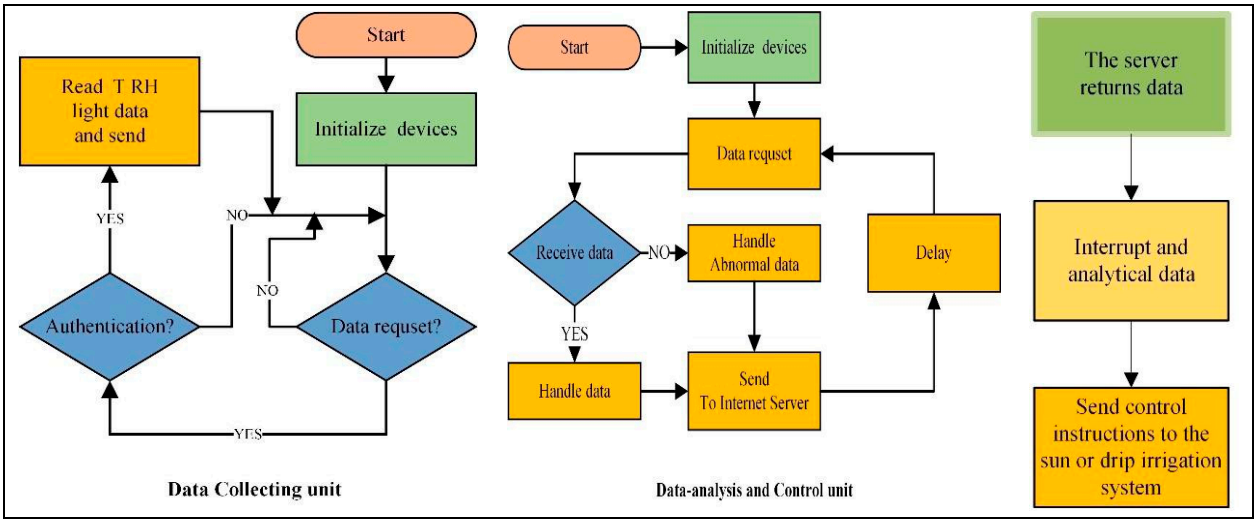

Figure 5. System software diagram.

2.3. Pot Structure

The structure of the pot where we plant vegetation is shown in Figure 6. As depicted, there exists three layers a soil layer, a cloth layer and a brick layer. The soil layer provides living substrate for vegetation and peat is adopted in our experiment. The cloth layer filters the water while preventing the soil from loss. The brick layer, which is composed of tiny brick and perlite, is capable of maintaining humidity as long as the substrate becomes dry. Besides, it can also drain water off quickly in case of rainstorm. The water tank underneath stores water for irrigation and avoids leak of water which is harmful for the structure of roofs. Sensors of temperature and humidity are placed between the soil layer and the cloth layer to provide information for substrate conditions. There are several species of plants,

including *Sedum sarmentosum* Bunge, *Lolium perenne* L., *Capsicum annuum* L. and *Portulaca grandiflora*, being tested for comparison. Local plants are adopted since they are well-adjusted to local environment.

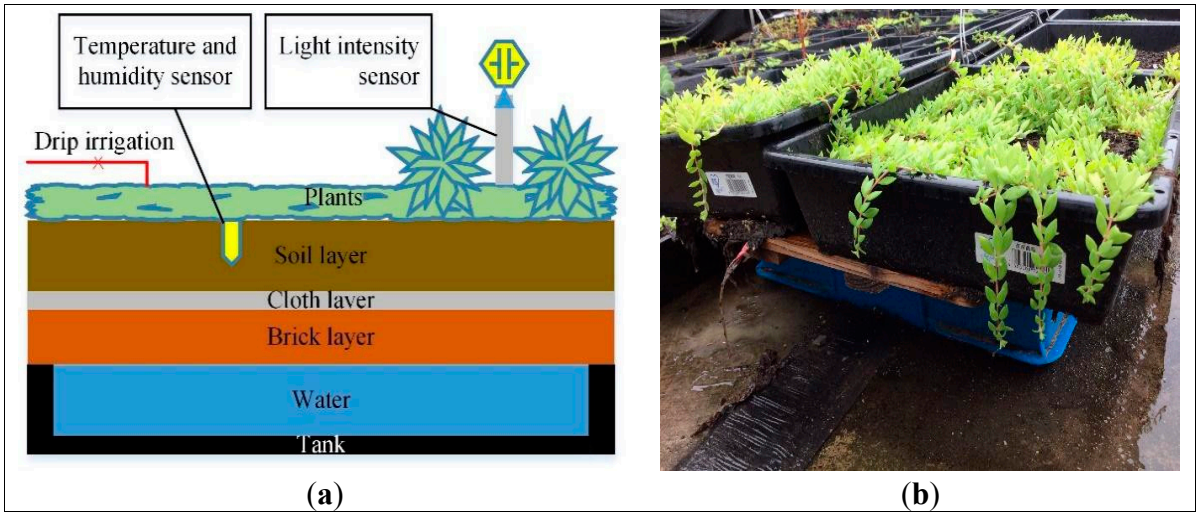

Figure 6. Pot structure. (**a**) Pot Prototype; (**b**) Pot implementation.

3. Experiment Setup

The experiment was conducted since 15 June 2014 which is the hottest season in China. Two sites, marked in red, are selected for measurements in Suzhou China, as given in Figure 7, and each site covers an area of 49 square (7 m × 7 m). The fields labeled with "Roof with GRM" and "Bare roof" denote site with and without our green roof system respectively. There is marginal difference between those two sites in terms of sun radiation, altitude and humidity so that site induced bias can be reduced as much as possible. One thing to note is that observed thermal effects are quite similar in the period of three month. For the sake of space, only out-coming in August is itemized in this paper.

Figure 7. The experiment location.

The experimental layout in the "Roof with GRM" is shown in Figure 8 where the depth of substrate are 3 cm, 6 cm and 9 cm respectively in our research since they are benchmarks in most studies. Pots, whose dimensions are 355 mm × 280 mm, are placed in each block and labeled in the form "*-**-*".

The category of plants is distinguished by the first number where 1 represents *Sedum sarmentosum* Bunge, 2 denotes *Lolium perenne* L., 3 is *Capsicum annuum* L. and 4 symbolizes *Portulaca grandiflora*. We have 108 pots totally in the "Roof with GRM". The following two characters denote management method where A is shadowed, B represents non-shadowed, b denotes irrigated, c means irrigated and siphoned, d denotes siphoned only and e is irrigated manually. By "siphoned", we mean that the water in the tank and the substrate is bridged so that the dry substrate is able to siphon water directly from the tank. Nevertheless, the syphon effect is quite slow and thus the automatic irrigation is still required. Automatic irrigation differs from the manual irrigation in terms of irrigation time and operation model. The former irrigates when necessary while the latter irrigates 3 times per day regularly. The final number indicates the depth of substrate and whether pine needle is covered. The ordered numbers 1 to 5 denote 3 cm depth, 6 cm depth, 3 cm with pine needle covered, 6 cm with pine needle covered and 9 cm with pine needle covered respectively.

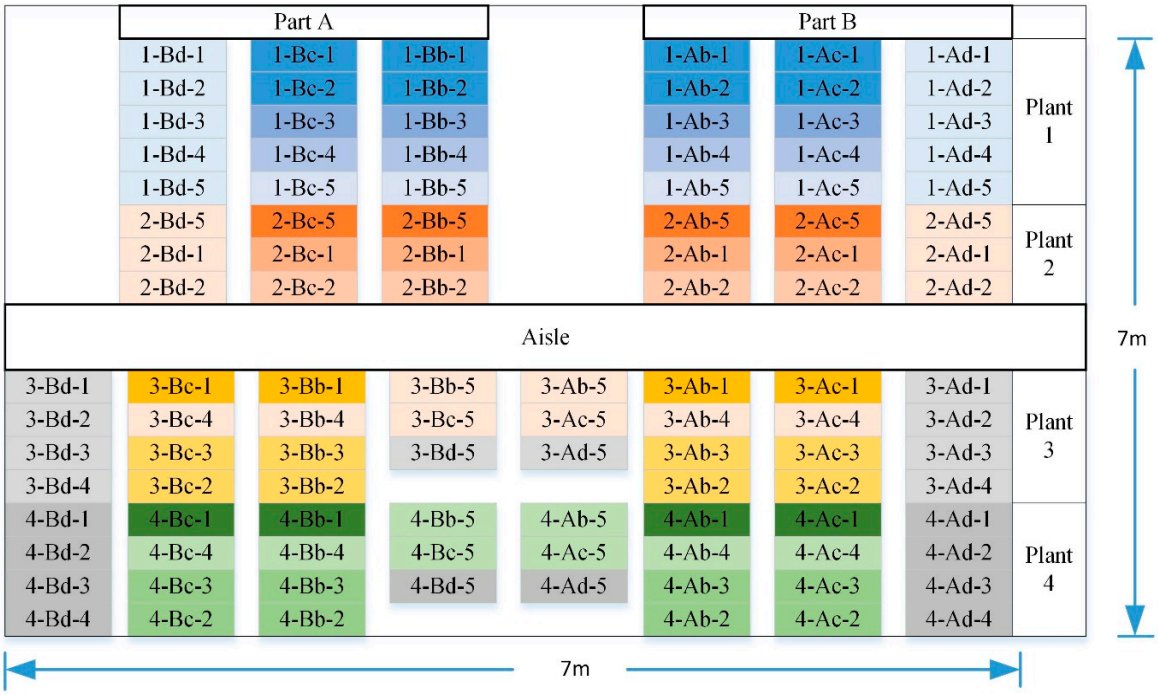

Figure 8. Experiment layout.

4. Results and Discussion

4.1. Survival Rate

Several parameters are proposed based on which the performance of the GRM system can be evaluated. Survival rate SR is the metric to indicate living conditions of plants and it is computed via

$$SR = \frac{SN}{TN} \tag{1}$$

where *SN* and *TN* denote the number of survived and total plants, final results are averaged and listed in Table 1.

Table 1. Survival rate.

	Non-Shadowed					**Shadowed**				
Plant	3 cm	3 cm + cover	6 cm	6 cm + cover	9 cm	3 cm	3 cm + cover	6 cm	6 cm + cover	9 cm
Sedum sarmentosum Bunge	61%	65%	68%	83%	95%	79%	82%	89%	100%	100%
Lolium perenne L.	62%	72%	88%	90%	99%	81%	91%	95%	100%	100%
Capsicum annuum L.	0	0	38%	40%	61%	0	17%	58%	82%	82%
Portulaca grandiflora	0	0	19%	28%	39%	0	6%	31%	49%	51%
	Non-irrigated					Irrigated				
	3 cm	3 cm + cover	6 cm	6 cm + cover	9 cm	3 cm	3 cm + cover	6 cm	6 cm + cover	9 cm
Sedum sarmentosum Bunge	61%	65%	68%	83%	95%	86%	98%	99%	100%	100%
Lolium perenne L.	62%	72%	88%	90%	99%	92%	97%	99%	100%	100%
Capsicum annuum L.	0	0	38%	40%	61%	65%	69%	74%	80%	100%
Portulaca grandiflora	0	0	19%	28%	39%	58%	63%	69%	79%	100%

As observed, *Sedum sarmentosum* Bunge as well as *Lolium perenne* L. are more drought-tolerant on average than *Capsicum annuum* L. and *Portulaca grandiflora* due to their plant characteristics. The shadowed vegetation outperforms those without shadowing in all cases. *Capsicum annuum* L. and *Portulaca grandiflora* are not able to survive in the 3 cm substrate whether or not it is shadowed. Nevertheless, 6% of *Portulaca grandiflora* and 17% of *Capsicum annuum* L. is able to survive if they are shadowed and covered. It increased dramatically when the depth of substrate increases to 6 cm for both *Capsicum annuum* L. and *Portulaca grandiflora* no matter shadowing is provided. The SR reaches as high as 58% for *Portulaca grandiflora* despite of its substrate depth of 3 cm if irrigation is offered. Other three plants out-behave *Portulaca grandiflora* in terms of survival rate. The SR continues growing, although the rate is not overwhelming, before reach 100%, demonstrating the outstanding performance of irrigation compared to shadowing. It is concluded that *Sedum sarmentosum* Bunge as well as *Lolium perenne* L. are preferred for roof greening due to their drought enduring nature and 9 cm is the optimal depth for the substrate.

4.2. Thermal Effects

Two sets of SHT11 sensors are deployed 10 cm high off both the bare roof and the green roof without shading after calibration to investigate the cooling effect of the plants.

A metric, termed *Bare-GR_Ratio* is defined as

$$Bare\text{-}GR\_Ratio = \frac{Bare - GR}{Bare} \tag{2}$$

where *GR* and *Bare* represent temperature obtained with and without the GRM system to evaluate the extent to which the green roof can improve the thermal conditions.

One more metric, denoted by *DEV*, is proposed to indicate the efficiency of the GRM in terms of thermal effects and it is derived via

$$DEV_i = x_i - (\sum_{j=1}^{M} x_j) / M \tag{3}$$

where x_i and x_j denote the ith and jth measurements respectively, and M is the number of measurements.

Figure 9 shows the temperature obtained in August 2014. As given in Figure 9a, the temperature on the bare ground tops at 47 °C in several days and bottoms at 28 °C in 17th August. Figure 9b reveals the absolute temperature decrease after the GRM system is implemented. As given, the GRM system is able to reduce as much as 8.4 °C and the average temperature decrease is 4.7 °C. On the contrary, Figure 9c outlines the comparative thermal condition improvement where the *Bare-GR_Ratio* fluctuates between 4.5% and 24% and averages at 12%. Figure 9d offers the thermal effects deviation derived from Equation (3). As seen, several points fall below the average temperature reduction levels and the key reason is that it is cloudy or rainy all these days.

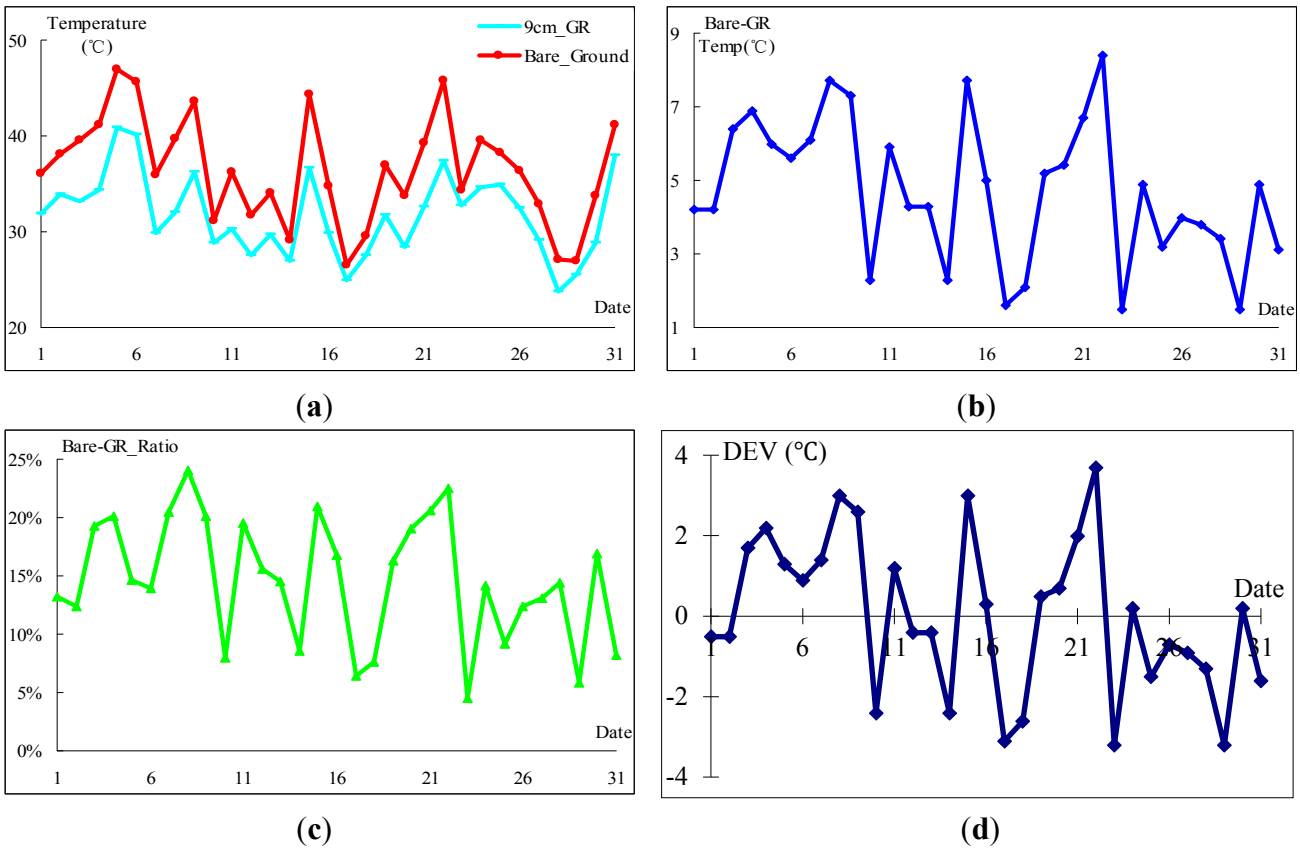

Figure 9. Thermal effect in the August. (**a**) Measured temperature; (**b**) Temperature reduction level; (**c**) Thermal improvement ratio; (**d**) Thermal effects deviation.

To explore the effects of the roof with GRM explicitly, we depict the thermal conditions on 24 August 2014 in Figure 10. It is clearly that the GRM system has positive cooling effect, especially at noon when the solar radiation is intensive. Figure 10b,c describes the absolute and comparative temperature reduction level of the GRM system. As outlined in Figure 10b, the graph stays between 1 °C and 7.8 °C and averages at 3.5 °C. The cooling effect tops from 13:00 to 16:00 when the outdoor temperature reaches its peak. Results in Figure 10c are obtained through Equation (2) where the *Bare-GR_Ratio* reminds stable initially until 08:00 and it climbs dramatically over the period of 08:00 and 12:00 before fluctuating in the following periods. Graph in Figure 10d are depicted using results computed via Equation (3). As seen, *DEV* stays below the average level stably before climbing up to 0, followed by a sharp increase, spanning from 10:00 to 13:00. Fluctuation is witnessed in the following

11 h with a downward trend and it stabilizes at 0 finally. To conclude, the thermal effects reach a peak at daytime.

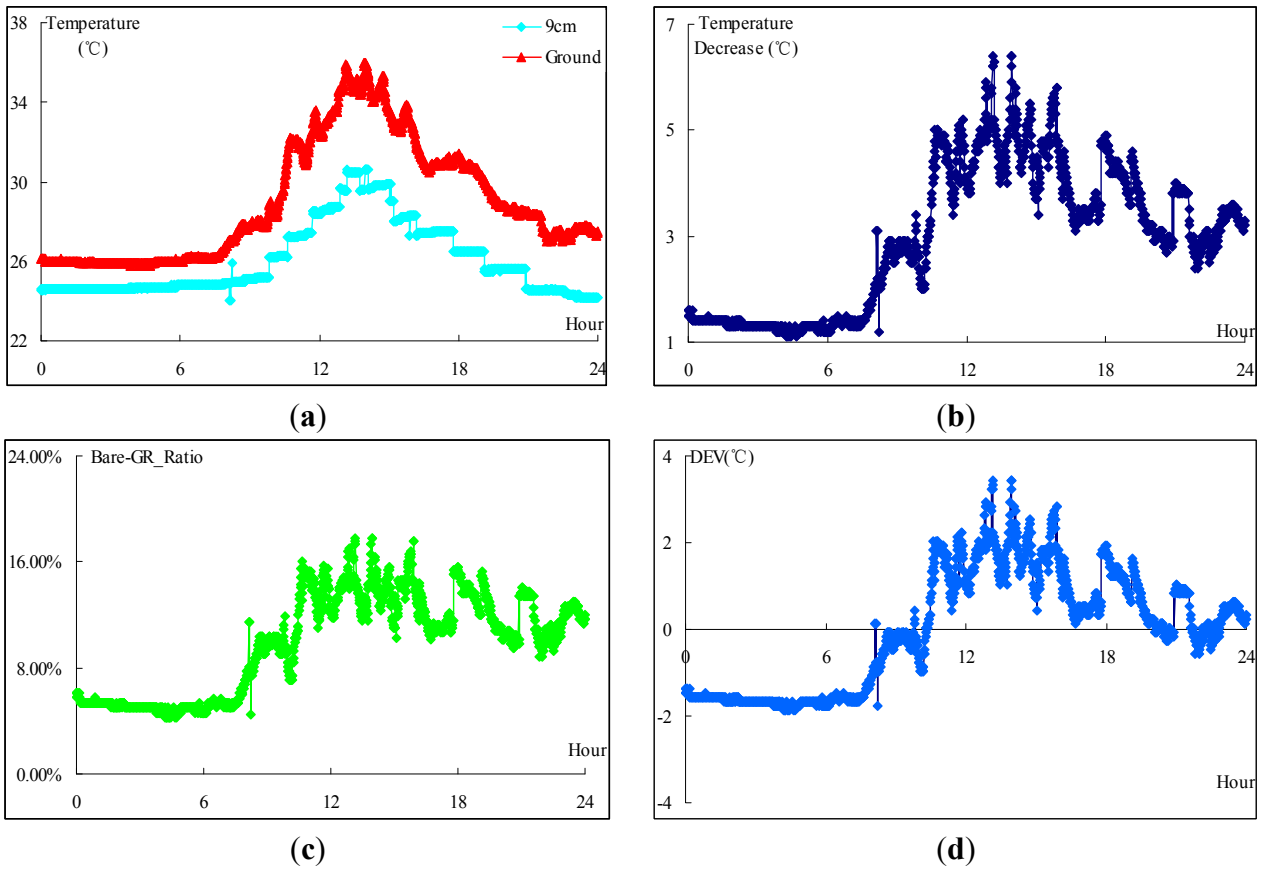

Figure 10. Thermal effect on August 24th. (**a**) Measured temperature; (**b**) Temperature reduction level; (**c**) Thermal improvement ratio; (**d**) Thermal effects deviation.

4.3. PM2.5 Reduction

The direct reading monitoring device, Dylos Air Quality Monitors (Model DC1700, with external dimensions of 17.78 cm × 11.43 cm × 7.62 cm) were deployed in two sampling roofs. Two sensors are calibrated beforehand to avoid initialization bias. Measurements are made 10 cm above the ground and the distance between two roofs is 30 m. Two sampling sites are strictly selected to ensure they are far from the PM2.5 sources. Figure 11 shows the density of PM2.5 in two sampling sites with and without the GRM system in 24 August 2014. Curves in both Figure 11a,b fluctuate over the sampling period. Graphs in Figure 11c,d are computed using Equations (2) and (3) respectively. Graph in Figure 11c reminds at the same level except that in the period from 06:00 to 09:00 where it plateaus at 20%. The DEV in Figure 11d fluctuates around the average level. These results suggest that the GRM system may improve air quality in terms of PM2.5 density. Further experiments are needed to confirm this finding, evaluate the local impact of the reduction, and evaluate the role of leaf area in PM removal.

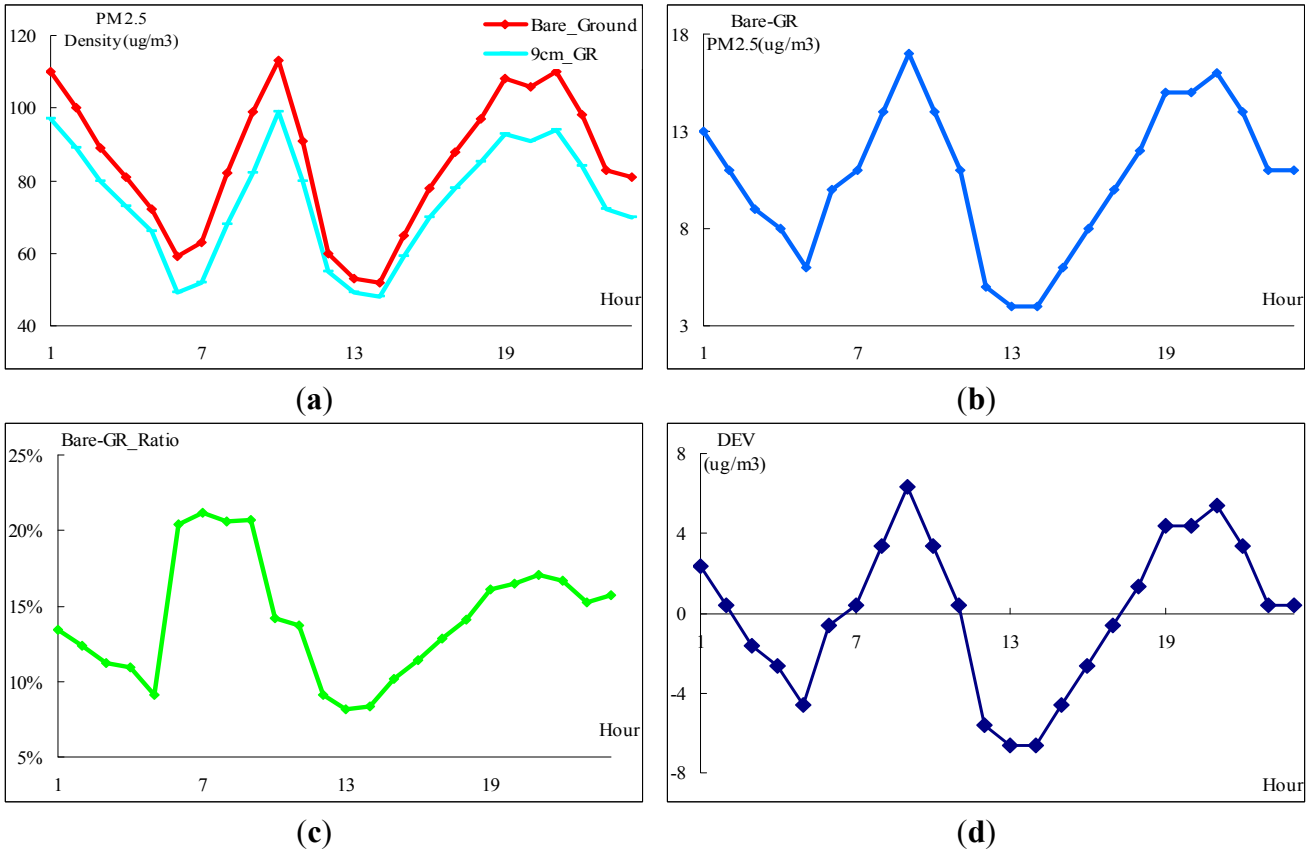

Figure 11. Density of PM2.5 with and without the GRM system. (**a**) Measured PM2.5 density; (**b**) PM2.5 reduction level; (**c**) PM2.5 density improvement ratio; (**d**) PM2.5 density deviation.

5. Conclusions and Future Work

A green roof system, termed the GRM, is introduced in this paper and its performance on the environment is studied. All electrical devices in this system operate on solar energy, which avoids additional energy cost. Rain is stored in this tank for irrigation when necessary. Results show that *Sedum sarmentosum* Bunge as well as *Lolium perenne* L. are more likely to survive compared to *Capsicum annuum* L. and *Portulaca grandiflora*.

An experiment was carried out, resulting in the observation that the GRM system is able to reduce as much as 15% degrees on average. A one day analysis shows that the GRM is capable of maintaining temperature between 24 °C and 28 °C reliably which is an ideal thermal environment for human beings. Besides, the effect of the GRM system on the local outdoor air quality was also exploited. Records validate the air quality improvement, although marginal, after deploying the GRM system.

The performance of the proposed green roof system is tested and validated in the horizontal roof. The thermal effect of the GRM may be significantly improved if shrubs are used due to their height and better shadowing effect compared with the low-growing vegetation adopted in this paper. One thing to note is that the growing pot, where vegetation is planted, is quite light and it may be blown away by strong wind which is quite dangerous, especially in high buildings. One method to solve this problem is to combine all growing pots together so that it can survive in a windstorm. In the future, we will

investigate the effect of the GRM on the biodiversity in the city and experiments are still required regarding its applications in tilted roofs.

Acknowledgments

The project was supported by the National Science Foundation Fund (61401297), Jiangsu Science Foundation Fund (BK20140283), Suzhou Science and Technology Fund (SZS201304, SYG201255), Jiangsu Key Laboratory of Intelligent Building Energy Efficiency, Suzhou key laboratory of mobile networking and applied technologies (SZS201304-3), Key Lab of Nanodevices and Nanoapplications, Suzhou Institute of Nano-Tech and Nano-Bionics, CAS (14ZS05) and Suzhou Bureau of Housing and Urban-Rural Development.

Author Contributions

All authors participated in the literature review and writing of this manuscript. Heng Luo was responsible for research planning and performance evaluation of the system. Jianping Chen was responsible for the data analysis. Ning Wang and Xiaoyan Ye designed and tested the whole irrigation and shading system. Yun-Fei Sun was responsible for chip design and analysis.

Conflicts of Interest

The authors declare no conflict of interest.

References

1. Miller, K.A.; Siscovick, D.S.; Sheppard, L.; Shepherd, K.; Sullivan, J.H.; Anderson, G.L.; Kaufman, J.D. Long-term exposure to air pollution and incidence of cardiovascular event in woman. *N. Engl. J. Med*. **2007**, *356*, 447–458.
2. Kunzli, N.; Mudway, I.S.; Götschi, T.; Shi, T.; Kelly, F.J.; Cook, S.; Burney, P.; Forsberg, B.; Gauderman, J.W.; Hazenkamp, M.E.; *et al.* Comparison of oxidative properties, light absorbance, and total and elemental mass concentration of ambient PM2.5 collected at 20 European sites. *Environ. Health Perspect*. **2006**, *114*, 684–690.
3. Peters, A.; Veronesi, B.; Calderón-Garcidueñas, L.; Gehr, P.; Chen, L.C.; Geiser, M.; Reed, W.; Rothen-Rutishauser, B.; Schürch, S.; Schulz, H. Translocation and potential neurological effects of fine and ultrafine particules a critical update. *Part. Fibre Toxicol*. **2006**, *3*, 1–13.
4. Lin, R.S.; Sung, F.C.; Huang, S.L.; Gou, Y.L.; Ko, Y.C.; Gou, H.W.; Shaw, C.K. Role of urbanization and air pollution in adolescent asthma: A mass screening in Taiwan. *J. Formos. Med. Assoc*. **2001**, *100*, 649–655.
5. Brunekreef, B. Estimation of long-term average exposure to outdoor air pollution for a cohort study on mortality. *J. Expo. Anal. Environ. Epidemiol*. **2001**, *11*, 459–469.
6. Brunekreef, B.; Holgate, S.T. Air pollution and health. *Lancet* **2002**, *360*, 1233–1242.

7. Shahbaz, M.; Lean, H.H. Does financial development increase energy consumption? The role of industrialization and urbanization in Tunisia. *Energy Policy* **2012**, *40*, 473–479.
8. Poumanyvong, P.; Kaneko, S. Does urbanization lead to less energy use and lower CO_2 emissions? A cross-country analysis. *Ecol. Econ*. **2010**, *70*, 434–444.
9. Rizwan, A.M.; Dennis, L.Y.C.; Liu, C. A review on the generation, determination and mitigation of Urban Heat Island. *J. Environ. Sci*. **2008**, *20*, 120–128.
10. Yuan, F.; Bauer, M.E. Comparison of impervious surface area and normalized difference vegetation index as indicators of surface urban heat island effects in Landsat imagery. *Remote Sens. Environ*. **2007**, *106*, 375–386.
11. Streutker, D.R. Satellite-measured growth of the urban heat island of Houston, Texas. *Remote Sens. Environ*. **2003**, *85*, 282–289.
12. Ihara, T.; Kikegawa, Y.; Asahi, K.; Genchi, Y.; Kondo, H. Changes in year-round air temperature and annual energy consumption in office building areas by urban heat-island countermeasures and energy-saving measures. *Appl. Energy* **2008**, *85*, 12–25.
13. Hassid, S.; Santamouris, M.; Papanikolaou, N.; Linardi, A.; Klitsikas, N.; Georgakis, C.; Assimakopoulos, D.N. The effect of the Athens heat island on air conditioning load. *Energy Build*. **2000**, *32*, 131–141.
14. Daly, H.E. Toward some operational principles of sustainable development. *Ecol. Econ*. **1990**, *2*, 1–6.
15. Hopwood, B.; Mellor, M.; O'Brien, G. Sustainable development: Mapping different approaches. *Sustain. Dev*. **2005**, *13*, 38–52.
16. Durhman, A.K.; Rowe, D.B.; Rugh, C.L. Effect of watering regimen on chlorophyll fluorescence and growth of selected green roof plant taxa. *HortScience* **2006**, *41*, 1623–1628.
17. Fioretti, R.; Palla, A.; Principi, L.G. Green roof energy and water related performance in the Mediterranean climate. *Build. Environ*. **2010**, *45*, 1890–1904.
18. Ouldboukhitine, S.E.; Belarbi, R.; Jaffal, I.; Trabelsi, A. Assessment of green roof thermal behavior: A coupled heat and mass transfer model. *Build. Environ*. **2011**, *46*, 2624–2631.
19. Vanuytrecht, E.; van Mechelen, C.; van meerbeek, K.; Willems, P.; Hermy, M.; Raes, D. Runoff and vegetation stress of green roofs in a climate change perspective. *Landsc. Urban Plan*. **2014**, *122*, 68–77.
20. Madre, F.; Vergnes, A.; Machon, N.; Clergeau, P. A comparison of 3 types of green roof as habitats for arthropods. *Ecol. Eng*. **2013**, *57*, 109–117.
21. Madre, F.; Vergnes, A.; Machon, N.; Clergeau, P. Green roof as habitats for wild plant species in urban landscapes: First insights from a large-scale sampling. *Landsc. Urban Plan*. **2014**, *122*, 100–107.
22. Oberndorfer, E.; Lundholm, J.; Bass, B.; Coffman, R.R.; Doshi, H.; Dunnett, N.; Gaffin, S.; Köhler, M.; Liu, K.K.Y.; Rowe, B. Green roofs as urban ecosystems: Ecological structures, functions, and services. *BioScience* **2007**, *57*, 823–833.
23. Van Mechelen, C.; Dutoit, T.; Kattge, J.; Hermy, M. Plant trait analysis delivers an extensive list of potential green roof species for Mediterranean France. *Ecol. Eng*. **2014**, *67*, 48–59.

24. Van Mechelen, C.; Dutoit, T.; Hermy, M. Mediterranean open habitat vegetation offers great potential for extensive green roof design. *Landsc. Urban Plan*. **2014**, *121*, 81–91.